

000 BEYOND NEXT-TOKEN PREDICTION: DIFFUSION VS. 001 AUTOREGRESSIVE REASONING IN LLMs 002

003 **Anonymous authors**
004

005 Paper under double-blind review
006

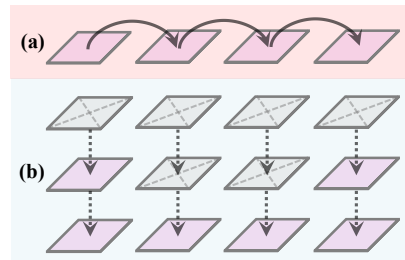
007 ABSTRACT 008

009 We revisit LLM reasoning through two competing decoding paradigms: au-
010 toregressive large language models (AR LLMs) with next-token prediction, and
011 diffusion-based large language models (DLLMs) with iterative denoising; yet
012 the community lacks compute-controlled, apples-to-apples comparisons. We re-
013 cast reasoning as trajectory formation, contrasting sequential commitment in AR
014 LLMs with iterative refinement in DLLMs, and run a matched-scale study across
015 mathematics, logic, natural-language inference, and commonsense QA, with ro-
016 bustness and efficiency analyses. Empirically, DLLMs outperform AR LLMs
017 on most reasoning benchmarks, especially those requiring global constraints
018 and long-range coherence, whereas AR LLMs remain competitive on shorter,
019 commonsense-oriented tasks. Mechanistic analyses show DLLMs gradually cor-
020 rect early errors and enforce sequence-wide consistency; robustness experiments
021 reveal graceful degradation under prompt noise and distribution shift. We quantify
022 accuracy-efficiency trade-offs: DLLMs increase FLOPs and wall-clock latency;
023 compute-matched comparisons preserve their advantage, indicating benefits arise
024 from the generative mechanism rather than added budget. Ablation studies further
025 reveal the influence of diffusion-specific design factors and demonstrate how these
026 parameters affect reasoning performance. While DLLMs incur higher inference
027 cost, our results delineate regimes where diffusion decoding is advantageous and
028 provide practical guidance for model configuration under deployment constraints.
029

030 1 INTRODUCTION 031

032 Large language models (LLMs) have shown strong rea-
033 soning across a wide range of tasks. Mainstream systems
034 (*e.g.*, GPT-4 (Achiam et al., 2023), Llama (Touvron et al.,
035 2023), Mistral (Jiang et al., 2023), and DeepSeek (Dai et al.,
036 2024)) use *next-token prediction* with autoregressive, left-
037 to-right decoding. Formally, an AR LLM factorizes the se-
038 quence probability into conditional next-token terms and is
039 trained with token-level cross-entropy. This design scales
040 well, aligns with hardware and streaming constraints, and
041 yields predictable inference latency, especially at scale. Yet
042 its virtues also crystallize failures: early choices are irre-
043 versible, exposure bias compounds along the chain, and lo-
044 cal normalization can induce “myopia,” *i.e.*, steps that are
045 locally plausible but globally inconsistent. Recent *de facto*
046 Chain-of-Thought supervision helps by injecting intermedi-
047 ate reasoning, but the underlying process still predicts one
048 token at a time (see Fig. 1(a)).

049 Inspired by the success of their counterparts in other domains, DLLMs (Li et al., 2022; Karimi Ma-
050 habadi et al., 2024) are emerging as a compelling alternative for reasoning. Instead of generating
051 text sequentially like autoregressive models, a diffusion-style model starts from noise and iteratively
052 denoises a representation toward a high-probability sequence (see Fig. 1(b)). If AR decoding is like
053 “speaking,” DLLM is like “editing,” allowing the model to revise its reasoning trajectory. This pro-
vides two key theoretical advantages: reversibility, where late steps can correct early mistakes, and



054 Figure 1: (a) **Autoregressive generation**: outputs are produced sequen-
055 tially \rightarrow one token  at a time.
056 (b) **Diffusion-based generation**: text is gradually refined from noise  through iterative \rightarrow denoising steps.
057

054 coarse-to-fine planning, which allows the model to first establish the high-level structure before filling
 055 in details. Recent scale-up DLLMs (Ye et al., 2025b; Nie et al., 2025) have shown this paradigm
 056 can match or even surpass AR baselines on general tasks. However, operational challenges remain,
 057 including a nuanced trade-off between quality and compute governed by discretization strategy,
 058 guidance strength, and so on, which directly impacts inference latency.

059 Despite significant momentum, the community lacks a timely and comprehensive analysis that compares
 060 these two paradigms specifically as mechanisms for reasoning, rather than just as alternative
 061 decoders. Existing reports (Ye et al., 2024; Deschenaux & Gulcehre, 2024; Feng et al., 2025; Gul-
 062 rajani & Hashimoto, 2023) vary widely in their benchmarking, metrics, and decoding schedules,
 063 making direct, apples-to-apples comparisons difficult. We therefore explicitly frame LLM reasoning
 064 as trajectory formation. In this view, AR LLMs construct a discrete trajectory with committed
 065 steps, while DLLMs iteratively refine a sequence of partially masked states via re-masking and
 066 resampling until convergence. This perspective enables a feasible, systematic comparison across ac-
 067 curacy, robustness, and efficiency. Motivated by this framework, we pose three research questions:

068 **RQ1:** *What* is the performance gap between autoregressive LLMs and DLLMs in reasoning
 069 across representative tasks under matched model scales?

070 **RQ2:** *When* do DLLMs outperform autoregressive LLMs, and *why*?

071 **RQ3:** *What* settings (e.g., guidance strength, schedule length, discretization and related param-
 072 eters) enable DLLMs to facilitate their performance across different winning scenarios?

073
 074 These research questions **comprehensively review DLLM**, as a new alternative to AR LLM, high-
 075 lighting its methodological distinctions, practical advantages, and potential to reshape future direc-
 076 tions in LLM reasoning. Our contributions and anticipated benefits include: ① **A first-of-its-kind**
 077 **same-scale evaluation.** We perform a systematic, same-scale comparison of DLLMs and AR LLMs
 078 of similar size (7~8B) across 20 diverse reasoning tasks. Our findings reveal that DLLMs yield
 079 higher accuracy on tasks requiring global constraints, while LLMs remain competitive on simpler
 080 commonsense QA. This work provides an empirical guide on when DLLMs offer gains and when
 081 AR LLMs is sufficient, thus supporting informed model choice under deployment needs. ② **An em-
 082 pirical analysis of DLLM's advantages.** Through fine-grained case studies, we provide an analysis
 083 of why DLLMs outperform LLMs on certain benchmarks. Our findings show that DLLMs' iterative
 084 refinement effectively corrects errors, enforces sequence-wide consistency, and avoids local traps
 085 that mislead LLMs. Furthermore, we demonstrate that DLLMs are more robust to prompt noise and
 086 distribution shift, revealing that their parallel refinement paradigm enables a level of robustness and
 087 global coherence that is inherently difficult to achieve with AR decoding. ③ **Systematic insights**
 088 **into efficiency and design.** We present a detailed investigation into the key design parameters of
 089 DLLMs, including remasking strategy, guidance strength, and schedule length, along with their
 090 computational and latency trade-offs. The results show that DLLM's performance is maintained in
 091 compute-matched settings. This provides a practical guide with principles for balancing accuracy
 092 and latency and identifies where diminishing returns begin to appear in the design space.

093 In short, this paper presents a head-to-head comparison of autoregressive and diffusion-based
 094 paradigms for reasoning. The rest of the paper is organized as follows. In §2, we review relevant lit-
 095 erature. We then provide some preliminary knowledge regarding the two LLM reasoning paradigms
 096 in §3. Our major empirical analysis is presented in §4~5, and we conclude with a discussion and an
 097 outlook on future work in §7.

098 2 RELATED WORK

100 2.1 AUTOREGRESSIVE REASONING

102 Autoregressive large language models (AR LLMs) decode left-to-right, predicting one token at a
 103 time conditioned on the current prefix (Vaswani et al., 2017; Brown et al., 2020; Tovvron et al., 2023;
 104 Jiang et al., 2023; Du et al., 2022). The procedure is operationally simple and hardware-efficient:
 105 computation factorizes into a chain of conditional predictions, latency grows approximately linearly
 106 with sequence length, and mature serving stacks deliver high throughput at scale (Narayanan et al.,
 107 2021; Rajbhandari et al., 2020; Korthikanti et al., 2022). As a result, AR decoding is the efficiency
 108 baseline for long-form inference (Achiam et al., 2023).

108 The same sequential commitment creates characteristic liabilities (Finlayson et al., 2024). Because
 109 decoding is unidirectional and effectively irreversible, early missteps propagate forward and are
 110 hard to repair; small local slips can induce long-range inconsistencies and brittle chains of reasoning
 111 (Schmidt, 2019; Ranzato et al., 2016; Bengio et al., 2015). Contemporary practice therefore leans
 112 on methods such as *test-time scaling*: spending additional inference compute to sample multiple
 113 rollouts, elicit intermediate steps, rerank candidates, or verify solutions with external checks (Wang
 114 et al., 2025b; Yu et al., 2025; Kumar et al., 2025; Hao et al., 2025; Chen et al., 2024; Joshi et al.,
 115 2025; Hao et al., 2025). These procedures improve robustness but remain auxiliary to the core
 116 mechanism—they patch rather than remove the fragility of strictly sequential next-token prediction
 117 (Zhang et al., 2023; 2024c). Conceptually, AR reasoning resembles human System 1, which aims
 118 for fast and intuitive responses when the initial trajectory is sound, yet vulnerable to systematic error
 119 when early cues mislead (Chang et al., 2024; Liu & Thoma, 2024; Wu et al., 2024b).

120 2.2 DIFFUSION-BASED REASONING

121 Diffusion-based language models (DLLMs) introduce a distinct generative paradigm centered on
 122 iterative denoising at inference (Sahoo et al., 2024; Chung et al., 2025; Do et al., 2025; Zheng
 123 et al., 2023; Austin et al., 2021; He et al., 2023). In contrast to one-pass AR decoding, DLLMs
 124 update multiple positions in parallel and repeatedly reconsider the global structure of their output.
 125 This provides a principled mechanism for self-correction, allowing the model to overwrite earlier
 126 commitments when accumulating evidence contradicts them (Xu et al., 2025; Cardei et al., 2025; Wu
 127 et al., 2025; Sahoo et al., 2025). The annealed nature of the denoising process naturally facilitates a
 128 coarse-to-fine planning strategy, where early steps focus on high-level semantic structure and later
 129 steps fill in details (Zhou et al., 2024a; Karimi Mahabadi et al., 2024; Huang & Tang, 2025). This
 130 hierarchical refinement is particularly advantageous for tasks requiring long-range planning, where
 131 a global understanding is critical to avoiding local inconsistencies (Lovelace et al., 2023; Xiong
 132 et al., 2024). The ability to revisit and revise any part of the sequence provides a powerful new tool
 133 for robust and controllable generation, transcending the immutable, left-to-right approach of AR
 134 LLMs (Han et al., 2023; Varma et al., 2025; Wang et al., 2025c). Recent large-scale systems extend
 135 DLLMs to multimodal and instruction-following settings (Yang et al., 2025; Zhu et al., 2025a; You
 136 et al., 2025), showing the paradigm’s versatility. These DLLMs fall into two primary families:
 137 discrete (based on mask tokens) and continuous (operating on latent spaces), with discrete models
 138 currently dominating in performance. For our work, all compared DLLMs are of the discrete type.

139 Despite rapid progress, systematic, compute-matched comparisons between DLLMs and strong AR
 140 baselines on multi-step reasoning remain scarce. This paper offers a timely analysis: a controlled,
 141 side-by-side study of efficiency, accuracy, and failure modes that clarifies AR- versus diffusion-style
 142 reasoning paradigms, and distills implications for future research.

143 3 PRELIMINARIES

145 We view reasoning as *trajectory formation* conditioned on an input x (prompt) that yields an output
 146 sequence $y = (y_1, \dots, y_T)$. AR LLMs directly generate discrete tokens; DLLMs refine a continuous
 147 latent trajectory (z_1, \dots, z_K) and then discretize to tokens.

149 3.1 AUTOREGRESSIVE LLMs

150 An AR LLM factorizes the conditional distribution as:

$$152 \quad p_{\theta}(y \mid x) = \prod_{t=1}^T p_{\theta}(y_t \mid x, y_{<t}), \quad (1)$$

155 and is trained by minimizing token-level cross-entropy,

$$157 \quad \mathcal{L}_{\text{CE}}(\theta) = -\mathbb{E}_{(x,y)} \sum_{t=1}^T \log p_{\theta}(y_t \mid x, y_{<t}). \quad (2)$$

160 Left-to-right decoding (e.g., greedy, beam, or stochastic sampling, optionally with post-training
 161 supplements, such as chain-of-thought prompting (Wei et al., 2022; Zhou et al., 2023; Kojima et al.,
 2022; Suzgun et al., 2023; Fu et al., 2023), test-time scaling (Wang et al., 2023b; Yao et al., 2023;

162 Cobbe et al., 2021; Wu et al., 2024b;a; Chen et al., 2024; Wang et al., 2025d; Knappe et al., 2024;
 163 Yu et al., 2025; Kumar et al., 2025; Zhang et al., 2024b; Joshi et al., 2025)) is *commitment-based*:
 164 once a token is emitted, later steps condition on it, which yields scalability and streamability while
 165 making early mistakes hard to repair without external search.

166 For cost intuition, if L denotes the number of generated tokens (including any CoT-like attempts),
 167 S the number of independent samples, B the beam width, and V the number of verifier/reranking
 168 passes, a rough per-query accounting is:

$$\text{Cost}_{\text{AR}} \approx c_{\text{tok}} L (S + B + V), \quad (3)$$

170 with c_{tok} the per-token forward cost. Test-time scaling aligns naturally with this decomposition. The
 171 most well-known attempts are self-consistency (Wang et al., 2023b), which increases S and beam
 172 search, which enlarges B (Vijayakumar et al., 2018). Note that in our study, we exclude the results
 173 that AR LLMs trained with reinforcement learning (RL) for fair comparisons, as diffusion-based
 174 LLMs remain in an early stage (Christiano et al., 2017; Ouyang et al., 2022; Zelikman et al., 2022;
 175 Hao et al., 2025) and RL approaches for them are not yet sufficiently developed.

177 3.2 DIFFUSION-BASED LLMs

178 DLLMs are another visible path to achieve the intelligence exhibited by AR LLMs (Nie et al., 2025;
 179 Gong et al., 2025b): A forward masking process gradually replaces tokens in the original sequence
 180 x_0 with special [MASK] tokens (*i.e.*, M), producing a partially masked sequence x_t via:

$$181 \quad \mathcal{L}(\theta) \triangleq -\mathbb{E}_{t, x_0, x_t} \left[\frac{1}{t} \sum_{i=1}^L \mathbf{1}[x_t^i = \text{M}] \log p_{\theta}(x_0^i | x_t) \right], \quad (4)$$

184 Its text generation follows a reverse-time refinement $z_K \rightarrow z_0$ before a discretization map $y =$
 185 $g(z_0; x)$ yields tokens. Because refinement edits the whole latent, DLLM supports *global reorganization*
 186 and *backtracking* prior to discretization. Its inference cost scales primarily with the number
 187 of denoising steps K (and optional restarts R),

$$188 \quad \text{Cost}_{\text{Diff}} \approx c_{\text{step}} K R + c_{\text{disc}}, \quad (5)$$

189 where c_{step} is the per-step cost and c_{disc} the discretization overhead. In our study, we vary schedule
 190 length K and guidance under matched computational budgets (see §5) so that any observed gains
 191 reflect the pathway rather than the extra compute.

192 Notice the difference between the cost of AR LLMs (see Eq. 3) and DLLMs (see Eq. 5), we hold
 193 constant datasets, prompts, model size and evaluation scripts to set up a fair benchmark. To test their
 194 stability, we sweep AR knobs (*i.e.*, beam width, self-consistency samples) and diffusion knobs (*i.e.*,
 195 schedule length K , guidance scale) under controlled settings.

196 4 UNDER MATCHED SCALE, DLLMs OUTPERFORM AR LLMs ON MOST 197 REASONING TASKS BUT INCUR MUCH HIGHER COMPUTATIONAL LATENCY

200 Our investigation starts with experimental analysis to address **RQ1**, assessing differences in reasoning
 201 performance between AR and DLLMs. We outline the baselines and datasets used in this study,
 202 which also apply to address RQ2 (see §5).

203 **Baselines.** We evaluate AR and DLLMs of comparable scale (*i.e.*, 7~8B parameters). AR baselines
 204 include Llama 3.1 8B (Touvron et al., 2023), Mistral 8B (Jiang et al., 2023), and DeepSeek 7B (Dai
 205 et al., 2024). DLLM baselines are Dream 7B (Ye et al., 2025b) and LLaDA 8B (Gong et al., 2025a).

207 **Datasets.** Our evaluation covers 13 benchmarks, which span a total of 20 tasks across four representative
 208 categories: quantitative reasoning, logical consistency, semantic entailment, and common-
 209 sense QA, following prior surveys (Yu et al., 2024; Sprague et al., 2025). Among them, Minerva
 210 Math consists of 7 sub-tasks and ANLI is composed of 3 rounds, which we count separately as tasks.

211 For *mathematical reasoning*, we use GSM8K (Cobbe et al., 2021), MathQA (Amini et al., 2019),
 212 and Minerva Math (Hendrycks et al., 2021). For *natural language inference*, we include ANLI (Nie
 213 et al., 2020), MNLI, and RTE (Williams et al., 2018). For *logical reasoning*, we test on LSAT-LR
 214 and LogiQA-en (Liu et al., 2020). For *commonsense QA*, we consider COPA (Roemmele et al.,
 215 2011), PIQA (Bisk et al., 2020), OpenBookQA (Mihaylov et al., 2018), and HellaSwag (Zellers
 et al., 2020). All datasets are accessed via Hugging Face.

Evaluation Metrics. We use exact match accuracy for GSM8K, MathQA, and Minerva Math; classification accuracy for ANLI, MNLI, and RTE; and multiple-choice accuracy for LSAT-LR, LogiQA-en, COPA, PIQA, Hellaswag, and OpenBookQA. More details are shown in Appendix §S1.

Benchmark Results. DLLMs achieve consistent advantages on benchmarks that demand stronger global consistency reasoning. Their iterative refinement helps in complex reasoning (see §2.2), whereas AR LLMs follow a fast left-to-right pathway, which remains competitive on simpler commonsense tasks. This motivates the deeper mechanism analyses in §5. In Fig. 2, we present the overall trends of AR LLMs and DLLMs, reporting average performance derived from AR LLMs and three DLLMs evaluated over 20 tasks. As seen, DLLMs average outperform AR counterparts on the majority of benchmarks, achieving higher accuracy on **16 of 20** tasks (e.g., GSM8K, MathQA, LogiQA, ANLI, MNLI). AR LLMs remain competitive on a smaller subset of commonsense QA tasks (e.g., PIQA, COPA, OpenBookQA, and Hellaswag). This demonstrates a clear performance gap in favor of diffusion decoding under matched model scales. On average, DLLMs improve accuracy by ~ 12 points over comparable AR LLMs under matched scale. For completeness, Appendix §S2 provides the detailed results of *each individual* AR LLM and DLLM, where the trend remains consistent.

Computational Efficiency Results.

We further report FLOPs/token, average output length, throughput, and latency in Table 1. As seen, DLLMs require higher computational cost per token than AR baselines (e.g., 16,120 GFLOPs/token for Dream-7B vs. 15 GFLOPs/token for Llama-3.1-8B), and also produce slightly longer outputs on average. Throughput is correspondingly low, with DLLMs generating only ~ 0.1 samples/s compared to 1.8–2.5 samples/s for AR LLMs. Latency comparisons further confirm this gap: diffusion decoding is consistently slower, often by $10\times$ – $200\times$ depending on the number of denoising steps (e.g., on GSM8K, Dream-7B is $25.9\times$ slower and LLaDA-8B is $27.4\times$ slower). All these trends stem from the DLLMs’ iterative refinement process, which demands many denoising steps per output. AR, on the other hand, is highly efficient, producing sequences in a single forward pass with much higher throughput. This highlights the key bottleneck of current DLLMs: while they improve reasoning accuracy, their practical deployment is constrained by computational efficiency. For completeness, results on other tasks are shown in Appendix §S5.

Chain-of-thought (CoT) Prompting Results.

Among post-training methods, CoT prompting is widely adopted to improve reasoning in AR LLMs (Wei et al., 2022). We thus naturally extend CoT to DLLMs, and evaluate CoT+AR LLMs’ and CoT+DLLMs’ performance, respectively.

Following prior work showing that mathematical reasoning benchmarks most clearly reveal the benefits of CoT prompting (Sprague et al., 2025), we evaluate their performance on the GSM8K (Cobbe et al., 2021) and Minerva Math (Hendrycks et al., 2021), which consists of 7 sub-tasks. As shown in Table 2, LLaDA (DLLM) shows a slight decrease in accuracy on both GSM8K and MATH, while Llama (AR) improves substantially on both benchmarks (e.g., +9 on GSM8K, +2 on MATH). These results demonstrate that CoT prompting yields substantially greater benefits for Llama than for LLaDA. These results highlight that DLLMs remain stronger in absolute terms, but AR LLMs benefit far more from CoT prompting. It suggests that DLLMs already rely on iterative refinement to

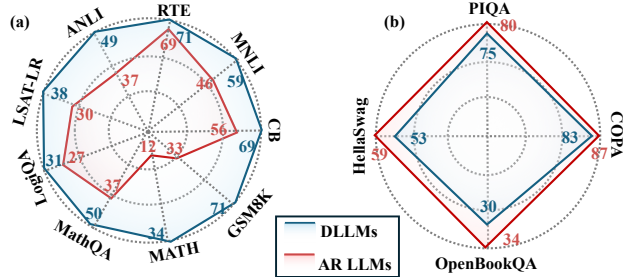


Figure 2: (a) **DLLMs** achieve higher accuracy on **math, logic, and NLI** benchmarks. (b) **AR LLMs** achieve higher accuracy on **commonsense QA**. Here, **MATH** refers to the Minerva MATH dataset (Hendrycks et al., 2021).

This motivates the deeper mechanism analyses in §5. In Fig. 2, we present the overall trends of AR LLMs and DLLMs, reporting average performance derived from AR LLMs and three DLLMs evaluated over 20 tasks. As seen, DLLMs average outperform AR counterparts on the majority of benchmarks, achieving higher accuracy on **16 of 20** tasks (e.g., GSM8K, MathQA, LogiQA, ANLI, MNLI). AR LLMs remain competitive on a smaller subset of commonsense QA tasks (e.g., PIQA, COPA, OpenBookQA, and Hellaswag). This demonstrates a clear performance gap in favor of diffusion decoding under matched model scales. On average, DLLMs improve accuracy by ~ 12 points over comparable AR LLMs under matched scale. For completeness, Appendix §S2 provides the detailed results of *each individual* AR LLM and DLLM, where the trend remains consistent.

Table 1: **Computational efficiency** comparison on GSM8K. ↘ denotes DLLMs (same for Table 2~4).

Model	FLOPs/Token (GFLOPs)	Avg. Tokens per Answer	Throughput (samples/s)	Latency (vs. Llama)
Dream-7B ↘	16,120 ¹	55.18	0.101	25.9×
LLaDA-8B ↘	19,590 ¹	63.37	0.064	27.4×
Llama-3.1-8B	15.0	53.05	2.49	1.0×
Mistral-7B	14.2	57.44	1.85	0.5×
DeepSeek-7B	14.0	54.77	1.92	0.4×

Table 2: **Effect of CoT prompting.**

Model	GSM8K		MATH	
	w/o CoT	w/ CoT	w/o CoT	w/ CoT
LLaDA-8B ↘	70.7	70.4	31.5	28.0
Llama-3.1-8B	49.9	58.8	18.2	20.1

270 enforce intermediate consistency, so additional explicit reasoning offers limited gains. By contrast,
 271 AR LLMs profit markedly from such external scaffolding, which helps mitigate their vulnerability
 272 to early commitment errors. More detailed CoT results are provided in Appendix S6.
 273

274 5 DLLMs OUTPERFORM AR LLMs ON GLOBAL-CONSTRAINT TASKS, 275 UNDER NOISY PROMPTS, AND AT MATCHED COMPUTATIONAL BUDGET

277 After establishing the overall performance study (RQ1), we turn to **RQ2**, analyzing when DLLMs
 278 outperform AR LLMs and further ask why. We first define the task taxonomy based on our evaluated
 279 datasets, and further observe three consistent patterns.

280 **Tasks Taxonomy.** In our study, we categorize tasks into two types: single-constraint and
 281 multi-constraint tasks. **Single-constraint tasks** generally require a single dominant decision
 282 guided by local cues. For example, the task is to choose the most plausible option in com-
 283 monsense QA benchmarks such as PIQA and COPA (see Appendix §S3). **Multi-constraint**
 284 **tasks**, on the other hand, require satisfying multiple interdependent constraints *jointly*. For
 285 instance, math tasks such as GSM8K and MATH demand consistency across intermediate vari-
 286 ables, where each step’s result must align with
 287 subsequent operations. Similarly, logical reasoning in LogiQA requires identifying which
 288 premises are relevant to the question and reasoning about their interrelations, ensuring
 289 consistency across multiple pieces of evidence.
 290 Natural language inference tasks such as ANLI further demand global semantic alignment be-
 291 tween premise and hypothesis, covering all
 292 relevant details rather than relying on surface
 293 overlap. In our study, while AR LLMs prefer single-constraint tasks (see Appendix S3), DLLMs
 294 achieve noticeable advantages in multi-constraint tasks (see **Finding I**).
 295

303 **Finding I: DLLMs win on global, multi-constraint consistency.** DLLMs achieve superior ac-
 304 curacy on tasks requiring *multi-constraint satisfaction* and *global coherence*, such as math with in-
 305 termediate bookkeeping, multi-premise logic, and sentence-pair entailment. DLLMs’ iterative de-
 306 noising updates the *entire sequence in parallel*, enabling repeated checks and repairs of cross-token
 307 dependencies. This allows the model to satisfy multiple constraints simultaneously (*e.g.*, content,
 308 numeric validity, logical structure), instead of committing early to a single trajectory. Concretely,
 309 we examine the strengths of DLLM reasoning compared to AR LLMs on three representative multi-
 310 constraint tasks (*i.e.*, mathematical reasoning, natural language inference, and logical reasoning).

311 As presented in Fig. 4, the example DLLM (*i.e.*, LLaDA) demonstrates its effectiveness in com-
 312 plying with multiple constraints where AR LLM (*i.e.*, Llama) fails to do so. **I.** On GSM8K, a
 313 mathematical reasoning benchmark of math word problems where multiple quantitative constraints
 314 are given, correct solutions require satisfying all given constraints simultaneously. In Fig. 4(a), AR
 315 LLM Llama neglects constraints 1 and 2, resulting in a fatal error that incorrectly calculates the cost
 316 of supplies for 20 candles, which finally leads to a completely wrong solution. In contrast, DLLM
 317 LLaDA successfully captures all the key quantitative constraints and produces a final correct solu-
 318 tion. **II.** On ANLI, a natural language inference benchmark where models must respect semantic
 319 and lexical constraints as well as factual boundaries established by the premise to make logically
 320 consistent inferences about the hypothesis, we observe similar patterns. The example in Fig. 4(b)
 321 demonstrates that Llama fails to comply with the lexical constraints, while LLaDA successfully
 322 detects the lexical inconsistency and predicts the correct answer. **III.** On a more challenging log-
 323 ical reasoning benchmark LogiQA, as shown in Fig. 4(c), Llama fails to satisfy spatial constraint

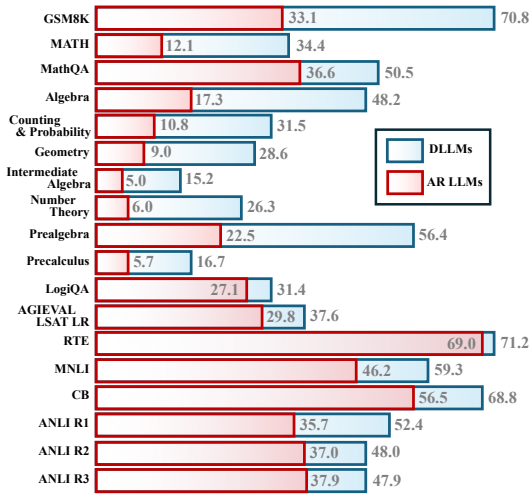


Figure 3: **DLLMs outperforms AR LLMs on tasks requiring multi-constraints**, including math reasoning, multi-premise logic, and NLI.

¹FLOPs data for Dream-7B and LLaDA-8B are reported from (Liu et al., 2025).

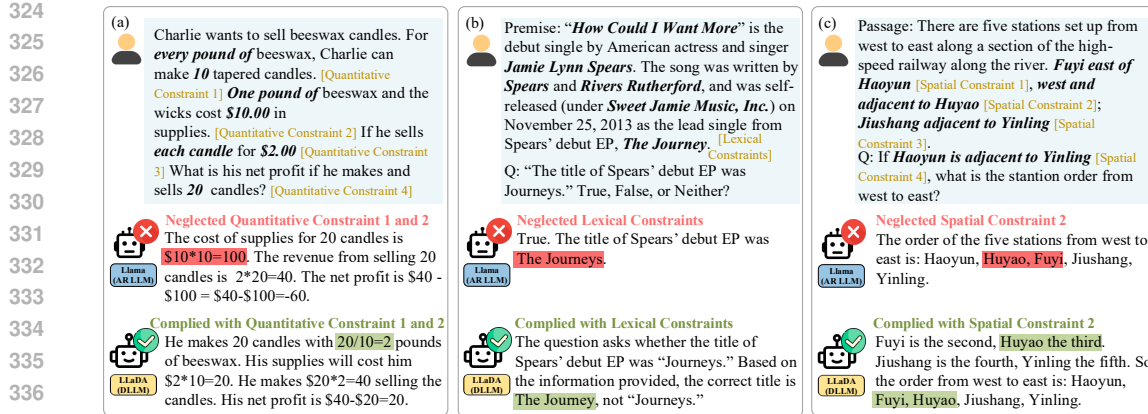


Figure 4: **Case analysis of AR LLM and DLLM on multi-constraint reasoning tasks.** Examples show AR LLM (Llama) failures due to constraint neglect on (a) GSM8K mathematical reasoning, (b) ANLI natural language inference, and (c) LogiQA logical reasoning. The colors indicate whether one or more constraints are **neglected** or **complied with** during the reasoning process.

2, leading to incorrect logical reasoning. In contrast, LLaDA captures all the logical cues and constraints, demonstrating superior constraint adherence. These observations highlight that DLLMs' parallel decoding mechanism provides robustness against constraint neglecting and multi-constraint satisfaction failures that AR LLMs suffer from. Additional cases are provided in Appendix S4.

Finding II: DLLMs are more robust to prompt noise. Under prefix and suffix perturbations, AR decoding couples tightly to corrupted input, causing small changes to cascade through the entire sequence. DLLMs, in contrast, *gradually correct* errors via multiple denoising steps under full context, enabling partial or strong recovery depending on noise severity.

To evaluate robustness, we construct a GSM8K subset where both Llama (AR LLM) and LLaDA (DLLM) solve all problems correctly under clean prompts, and then inject 15 randomly sampled adversarial tokens either before (*i.e.*, prefix) or after (*i.e.*, suffix) the query (Gan et al., 2024; Qiang et al., 2024; Anantheswaran et al., 2024). As shown in Table 3, results are evaluated on a GSM8K subset where both models are correct under clean prompts.

Under prefix and suffix noise attacks, Llama's accuracy collapses to 34%, while LLaDA maintains substantially higher robustness at 50%. This gap reflects the distinct error behaviors of the two paradigms under perturbations. DLLMs, though still affected by perturbations, can partially recover and preserve reasoning consistency, whereas AR LLMs are more tightly coupled to the injected noise. Under clean prompts, both models produce step-by-step arithmetic reasoning and correct answers. After injection, Llama often outputs an anomalously large spurious number as its first step and then rationalizes it, revealing irreversible error accumulation. By contrast, LLaDA maintains stable intermediate computations and recovers the correct answer (see Fig. 5). This suggests that iterative denoising mitigates perturbations and stabilizes the reasoning trajectory.

Overall, these results connect task demands with decoding dynamics: DLLM's parallel refinement favors tasks needing global consistency and robustness to perturbations, while AR's causal composition favors tasks reducible to a single left-to-right reasoning chain.

Finding III: DLLMs maintain their advantages under matched computational budget.

We further examine computational overhead using inference FLOPs. DLLMs inherently require multiple denoising iterations during decoding, resulting in higher computational demands compared to AR LLMs. To isolate the effects of model architecture from computational cost, we adopt the

Table 3: **Accuracies under noise perturbations.**

Model	Clean	Prefix	Suffix
LLaDA	100	68	50
Llama	100	31	36

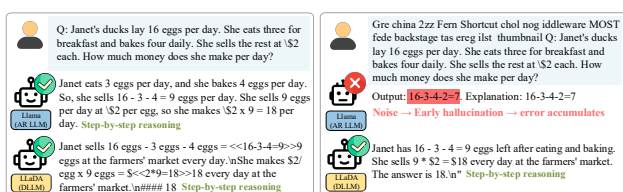


Figure 5: Adversarial noise triggers **AR LLMs error accumulation**, while **DLLM remains stable**

compute-matching setting from Wu et al. (2024a). In this controlled setting, AR LLM inference is executed multiple times via test-time scaling (Wang et al., 2023b; Wu et al., 2024a; Wang et al., 2025d), while LLaDA-8B (DLLM) are equipped with KV cache (Liu et al., 2025) matching the caching mechanism in Llama-3.1-8B (AR LLMs) to ensure a fair comparison. As shown in Table 4, we run $n = 140$ and $n = 560$ samples for Llama, aligned to 256 denoising steps and 512 steps with generate length 512 for LLaDA, respectively. Even under these matched-compute settings, LLaDA continue to consistently outperform Llama (*i.e.*, 74 vs. 68% at $1.0\times$, and 78% vs. 69% at $4.0\times$).

LLaDA delivers consistently higher accuracy than Llama. The advantage persists across budgets, showing that additional AR test-time sampling cannot close the gap. This finding underscores that DLLMs’ strengths come from their refinement mechanism rather than from extra computational resources. Due to computational resource limits, these matched-compute comparisons were conducted on a 100-example subset of GSM8K. We also tested alternative test-time scaling methods, such as beam search, but found that AR LLMs still underperform DLLMs. More details and results are provided in Appendix §S7.

Table 4: Accuracy under **matched compute resources**. \dagger LLaDA results are reported with KV cache.

Configuration	FLOPs	Acc. (%)
LLaDA-8B \dagger , 256 steps	$1.0\times$	74
Llama-3.1-8B, $n = 140$	$1.0\times$	68
LLaDA-8B \dagger , 512 steps + 512 gen	$4.0\times$	78
Llama-3.1-8B, $n = 560$	$4.0\times$	69

6 DLLMS REQUIRE STRUCTURED DISCRETIZATION, LONG SCHEDULES, AND BALANCED HYPERPARAMETERS

Table 5: **Ablation studies** for DLLM (LLaDA) on GSM8K. Unless otherwise specified, the default setting uses 256 denoising steps, generates length 256, block length 256, low-confidence masking, CFG 0.0, and temperature 0.0. The adopted designs are marked in red.

(a) Discretization		(b) Guidance		(c) Schedule		(d) Generate		(e) Block		(f) Temperature	
Scheme	Acc. (%)	Strength	Acc. (%)	Steps	Acc. (%)	Length	Acc. (%)	Block Size	Acc. (%)	Temp	Acc. (%)
Random	15.6	CFG 0.0	70.7	64 steps	40.5	256	70.7	256	70.7	0.0	70.7
LowConf	70.7	CFG 0.5	70.2	128 steps	61.2	512	69.3	128	69.0	0.2	71.1
—	—	CFG 1.0	65.5	256 steps	70.7	1024	47.2	64	68.4	0.7	68.9
—	—	CFG 1.5	61.3	—	—	—	—	—	—	1.0	68.1

We then answer **RQ3**, searching the hyperparameter trends for DLLMs to maximize their reasoning performance. Specifically, we conduct systematic ablations on GSM8K, varying discretization schemes, guidance strengths, denoising schedules, temperature, and sampling strategy, where we recognize that these factors directly control how DLLM refines sequences.

Discretization Strategy. Diffusion decoding refines sequences by repeatedly re-sampling a subset of tokens at each step. There are two common schemes: (i) *random masking*, where tokens are re-sampled uniformly at random regardless of model uncertainty, and (ii) *low-confidence masking*, where only tokens with the lowest predicted confidence are re-sampled (Li et al., 2022; Sahoo et al., 2024). Shown in Table 5(a), the low-confidence strategy consistently achieves strong accuracy (*e.g.*, 70% on GSM8K), whereas random masking collapses performance to 16%. This pattern demonstrates that DLLMs depend on *structured refinement*. Focusing updates on uncertain tokens enables the model to progressively repair errors without disturbing already correct tokens. In contrast, unstructured randomness introduces noise into stable regions, disrupting global coherence and breaking the refinement trajectory.

Classifier-free Guidance (CFG). CFG (Ho & Salimans, 2021; Li et al., 2022; Chung et al., 2025; Han et al., 2024) scales the conditional score against the unconditional one, controlling how strongly the model follows the prompt versus exploring alternative completions. As shown in Table 5(b), moderate guidance (*i.e.*, 0.0 – 0.5) preserves accuracy at 70%, while stronger guidance (*i.e.*, 1.0 – 1.5) reduces accuracy to 66–61%. *Why does strong guidance hurt?* High guidance amplifies already confident tokens overly, which in turn suppresses diversity and the model’s capacity for self-correction. As a result, early errors are reinforced instead of revised. Moderate guidance, in contrast, preserves a balance between following the prompt and leaving flexibility to repair mistakes, which is sufficient for DLLMs since its iterative process already enforces global consistency.

Denoising Schedule Length. A key advantage of DLLMs lies in their ability to correct errors through iterative denoising (Ye et al., 2025a; Zhao et al., 2025). As shown in Fig. 6, performance improves as the number of iteration steps increases.

432 At 64 steps, multiple mistakes
 433 remain, and the reasoning process
 434 is unstable to DLLM. At
 435 128 steps, most errors are elimi-
 436 nated, and the overall struc-
 437 ture becomes gradually coher-
 438 ent. At 256 steps, all errors
 439 are corrected, and the solution
 440 converges to the correct an-
 441 swer. This progression shows
 442 that DLLMs refine incomplete or faulty reasoning into coherent solutions through repeated denoising
 443 cycles. The number of steps determines the refinement depth. Too few leave many errors unre-
 444 solved, while additional iterations gradually enforce global consistency. As reported in Table 5(c),
 445 accuracy increases from 40.5% at 64 steps to 61.2% at 128 steps, and reaches 70.7% at 256 steps.
 446

447 **Generate Length.** Increasing the generate length L_g produces longer outputs but splits decoding
 448 into more blocks, thereby reducing refinement steps per block (Arriola et al., 2025). While the total
 449 denoising iterations remain constant, each block receives fewer updates, weakening local correc-
 450 tion. As shown in Table 5(d), accuracy peaks at $L_g=256$, whereas longer lengths gradually cause
 451 reasoning drift and steadily reduce overall coherence of the solution process.
 452

453 **Block Length.** The block length specifies the span of each local update. Table 5(e) shows that
 454 DLLM’s accuracy reaches the highest when the block length is set to 256. In this case, the generate
 455 and block lengths are identical, allowing the model to refresh the entire sequence per iteration. Under
 456 this setting, DLLM avoids semantic fragmentation and ensures that local updates remain consistent
 457 with the global context. Reducing the block length (e.g., 128 or 64) fragments the updates, which
 458 weakens coordination across reasoning steps and results in lower accuracies.
 459

460 **Temperature.** DLLM’s temperature regulates randomness in token sampling. At $T=0$, decoding is
 461 deterministic. At very high T (e.g., 0.7~1.0), outputs become unstable and reasoning drifts (Fin-
 462 layson et al., 2024; Renze, 2024; Shih et al., 2023; Chang et al., 2023; Zhang et al., 2024a). Shown in
 463 Table 5(e), a moderate value around 0.2 achieves best balance. It enables exploration of alternatives
 464 while maintaining coherence, allowing DLLM to fix local errors without losing track.
 465

466 Overall, the results indicate that DLLMs’ effectiveness is strongly shaped by parameter choices. It
 467 is important to adopt principled configurations to achieve reliable performance.
 468

469 7 DISCUSSION AND CONCLUSION

470 We distill our findings into immediate guidance for practitioners. Our analysis suggests that AR
 471 LLMs and DLLMs resemble computational analogues of *fast* and *slow* thinking, respectively: AR
 472 LLMs generate rapidly via greedy, token-by-token decoding (*i.e.*, System 1-like efficiency), whereas
 473 DLLMs iteratively refine a global representation (*i.e.*, System 2-like deliberation). We use this lens
 474 to analyze each paradigm’s characteristic strengths and liabilities in reasoning.
 475

476 The primary engineering challenge for DLLMs is computational cost. Iterative refinement is pow-
 477 erful but raises FLOPs and latency, limiting suitability under strict service-level constraints in pro-
 478 duction and large-scale serving contexts. Promising mitigation include step distillation (Chen et al.,
 479 2025; Xie et al., 2024; Salimans et al., 2024; Zhou et al., 2024b; Zhu et al., 2025b; Ho & Salimans,
 480 2022), rectified-flow and related training (Lee et al., 2024; Zhu et al., 2024; Lipman et al., 2023;
 481 Wang et al., 2025a), and consistency training (Song et al., 2023; Song & Dhariwal, 2024; Dao et al.,
 482 2025). In particular, learned step-size schedules and adaptive stopping criteria should be prioritized
 483 to tighten the quality-latency trade-off without eroding DLLMs’ capacity for global correction.
 484

485 Our evaluation also reveals a clear crossover regime. For tasks with short causal chains and tight
 486 latency budgets, AR LLMs tend to dominate; additional DLLM iterations add unnecessary delibera-
 487 tion and may even depress accuracy. Conversely, on problems with multi-variable dependencies and
 488 long-range coherence requirements, DLLMs excel by progressively enforcing global consistency
 489 and reducing internal contradictions. These results naturally motivate hybrid designs: use a two-
 490 stage pipeline where an AR LLM produces a draft and a DLLM refines it to enforce constraints and
 491 resolve inconsistencies, or adopt dynamic routing that estimates task difficulty online and selects the
 492 appropriate pathway, allocating compute where it yields the highest return.
 493

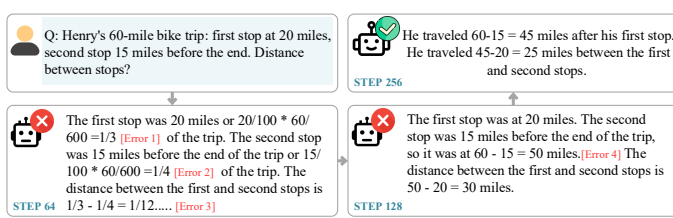


Figure 6: **Error correction** in DLLMs as denoising progresses.

486
487

ETHICS STATEMENT

488

We conform to the ICLR Code of Ethics and further show the consent to our work below. All datasets used in this study are publicly available and released under permissive licenses (see Appendix §S9), and all the models are publicly available (see Appendix §S9 for Asset License and Consent). We would like to state that the contents in the dataset do NOT represent our views or opinions and our paper does not involve crowdsourcing or research with human subjects.

489

490

REPRODUCIBILITY STATEMENT

491

492

All experiments in this paper are evaluation-only. Our implementation is based on PyTorch (Paszke et al., 2019) and runs on NVIDIA A100-40GB GPUs. We evaluate publicly available models on publicly available datasets (see Appendix §S9 for details). We provide exact dataset and evaluation metrics Appendix §S1, so that our reported results can be reproduced. Our evaluation scripts will be released upon acceptance.

493

494

REFERENCES

495

Josh Achiam, Steven Adler, Sandhini Agarwal, Lama Ahmad, Ilge Akkaya, Florencia Leoni Aleman, Diogo Almeida, Janko Altenschmidt, Sam Altman, Shyamal Anadkat, et al. Gpt-4 technical report. *arXiv preprint arXiv:2303.08774*, 2023.

496

497

Aida Amini, Saadia Gabriel, Peter Lin, Rik Koncel-Kedziorski, Yejin Choi, and Hannaneh Hajishirzi. MathQA: A new dataset for sub-challenge of AIs in answering math word problems. In *NAACL*, 2019.

498

499

Ujjwala Anantheswaran, Himanshu Gupta, Kevin Scaria, Shreyas Verma, Chitta Baral, and Swaroop Mishra. Cutting through the noise: Boosting llm performance on math word problems. In *ICLR*, 2024.

500

501

Marianne Arriola, Aaron Gokaslan, Justin T. Chiu, Zhihan Yang, Zhixuan Qi, Jiaqi Han, Subham Sekhar Sahoo, and Volodymyr Kuleshov. Block diffusion: Interpolating between autoregressive and diffusion language models. In *ICLR*, 2025.

502

503

Jacob Austin, Daniel D. Johnson, Jonathan Ho, Daniel Tarlow, and Rianne van den Berg. Structured denoising diffusion models in discrete state-spaces. In *NeurIPS*, 2021.

504

505

Samy Bengio, Oriol Vinyals, Navdeep Jaitly, and Noam Shazeer. Scheduled Sampling for Sequence Prediction with Recurrent Neural Networks. In *NeurIPS*, 2015.

506

507

Yonatan Bisk, Rowan Zellers, Ronan Lebras, Jianfeng Gao, and Yejin Choi. PIQA: Reasoning about physical commonsense in natural language. In *AAAI*, 2020.

508

509

Tom Brown, Benjamin Mann, Nick Ryder, Melanie Subbiah, Jared Kaplan, Prafulla Dhariwal, Arvind Neelakantan, Pranav Shyam, Girish Sastry, Amanda Askell, Sandhini Agarwal, Ariel Herbert-Voss, Gretchen Krueger, Tom Henighan, Rewon Child, Aditya Ramesh, Daniel Ziegler, Jeffrey Wu, Clemens Winter, Chris Hesse, Mark Chen, Eric Sigler, Mateusz Litwin, Scott Gray, Benjamin Chess, Jack Clark, Christopher Berner, Sam McCandlish, Alec Radford, Ilya Sutskever, and Dario Amodei. Language models are few-shot learners. In *NeurIPS*, 2020.

510

511

Michael Cardei, Jacob K Christopher, Thomas Hartvigsen, Brian R Bartoldson, Bhavya Kailkhura, and Ferdinando Fioretto. Constrained language generation with discrete diffusion models. *arXiv preprint arXiv:2503.09790*, 2025.

512

513

Chia-Hsuan Chang, Mary M. Lucas, Yeawon Lee, Christopher C. Yang, and Grace Lu-Yao. Beyond self-consistency: Ensemble reasoning boosts consistency and accuracy of llms in cancer staging. In *AIME*, 2024.

514

515

Chung-Ching Chang, David Reitter, Renat Aksitov, and Yun-Hsuan Sung. Kl-divergence guided temperature sampling. *arXiv preprint arXiv:2306.01286*, 2023.

- 540 Tianqi Chen, Shujian Zhang, and Mingyuan Zhou. Dlm-one: Diffusion language models for one-
 541 step sequence generation. *arXiv preprint arXiv:2506.00290*, 2025.
- 542
- 543 Xinyun Chen, Renat Aksitov, Uri Alon, Jie Ren, Kefan Xiao, Pengcheng Yin, Sushant Prakash,
 544 Charles Sutton, Xuezhi Wang, and Denny Zhou. Universal self-consistency for large language
 545 model generation. In *ICML*, 2024.
- 546 Paul Christiano, Jan Leike, Tom Brown, Miljan Martic, Shane Legg, and Dario Amodei. Deep
 547 reinforcement learning from human preferences. In *NeurIPS*, 2017.
- 548
- 549 Hyungjin Chung, Jeongsol Kim, Geon Yeong Park, Hyelin Nam, and Jong Chul Ye. CFG++:
 550 manifold-constrained classifier free guidance for diffusion models. In *ICLR*, 2025.
- 551
- 552 Karl Cobbe, Vineet Kosaraju, Mohammad Bavarian, Mark Chen, Heewoo Jun, Lukasz Kaiser,
 553 Matthias Plappert, Jerry Tworek, Jacob Hilton, Reiichiro Nakano, Christopher Hesse, and John
 554 Schulman. Training verifiers to solve math word problems. *arXiv preprint arXiv:2110.14168*,
 2021.
- 555
- 556 Damai Dai, Chengqi Deng, Chenggang Zhao, R. X. Xu, Huazuo Gao, Deli Chen, Jiashi Li,
 557 Wangding Zeng, Xingkai Yu, Y. Wu, Zhenda Xie, Y. K. Li, Panpan Huang, Fuli Luo, Chong
 558 Ruan, Zhifang Sui, and Wenfeng Liang. Deepseekmoe: Towards ultimate expert specialization in
 559 mixture-of-experts language models. In *ACL*, 2024.
- 560
- 561 Quan Dao, Khanh Doan, Di Liu, Trung Le, and Dimitris N. Metaxas. Improved training technique
 562 for latent consistency models. In *ICLR*, 2025.
- 563
- 564 Justin Deschenaux and Caglar Gulcehre. Promises, outlooks and challenges of diffusion language
 565 modeling. *arXiv preprint arXiv:2406.11473*, 2024.
- 566
- 567 Huu Dat Do, Duc Anh Do, Anh Tuan Luu, and Wray Buntine. Discrete diffusion language model
 568 for efficient text summarization. In *NAACL*, 2025.
- 569
- 570 Danny Driess, Fei Xia, Mehdi S. M. Sajjadi, et al. Palm-e: An embodied multimodal language
 571 model. In *ICML*, 2023.
- 572
- 573 Zhengxiao Du, Yujie Qian, Xiao Liu, Ming Ding, Jiezhong Qiu, Zhilin Yang, and Jie Tang. Glm:
 574 General language model pretraining with autoregressive blank infilling. In *ACL*, 2022.
- 575
- 576 Guhao Feng, Yihan Geng, Jian Guan, Wei Wu, Liwei Wang, and Di He. Theoretical benefit and
 577 limitation of diffusion language model. *arXiv preprint arXiv:2502.09622*, 2025.
- 578
- 579 Matthew Finlayson, John Hewitt, Alexander Koller, Swabha Swayamdipta, and Ashish Sabharwal.
 580 The curious case of neural text degeneration. In *ICLR*, 2024.
- 581
- 582 Yao Fu, Hao Peng, Ashish Sabharwal, Peter Clark, and Tushar Khot. Complexity-based prompting
 583 for multi-step reasoning. In *ICLR*, 2023.
- 584
- 585 Esther Gan, Yiran Zhao, Liying Cheng, Yancan Mao, Anirudh Goyal, Kenji Kawaguchi, Min-Yen
 586 Kan, and Michael Shieh. Reasoning robustness of llms to adversarial typographical errors. In
 587 *EMNLP*, 2024.
- 588
- 589 Shansan Gong, Shivam Agarwal, Yizhe Zhang, Jiacheng Ye, Lin Zheng, Mukai Li, Chenxin An,
 590 Peilin Zhao, Wei Bi, Jiawei Han, Hao Peng, and Lingpeng Kong. Scaling diffusion language
 591 models via adaptation from autoregressive models. In *ICLR*, 2025a.
- 592
- 593 Shansan Gong, Ruixiang Zhang, Huangjie Zheng, Jiatao Gu, Navdeep Jaitly, Lingpeng Kong, and
 594 Yizhe Zhang. Diffucoder: Understanding and improving masked diffusion models for code gen-
 595 eration. *arXiv preprint arXiv:2506.20639*, 2025b.
- 596
- 597 Ishaan Gulrajani and Tatsunori B. Hashimoto. Likelihood-based diffusion language models. In
 598 *NeurIPS*, 2023.
- 599
- 600 Cheng Han, James C Liang, Qifan Wang, Majid Rabbani, Sohail Dianat, Raghavveer Rao, Ying Nian
 601 Wu, and Dongfang Liu. Image translation as diffusion visual programmers. In *ICLR*, 2024.

- 594 Xiaochuang Han, Sachin Kumar, and Yulia Tsvetkov. Ssd-lm: Semi-autoregressive simplex-based
 595 diffusion language model for text generation and modular control. In *ACL*, 2023.
- 596
- 597 Qianyue Hao, Sibo Li, Jian Yuan, and Yong Li. RI of thoughts: Navigating llm reasoning with
 598 inference-time reinforcement learning. *arXiv preprint arXiv:2505.14140*, 2025.
- 599
- 600 Zhengfu He, Tianxiang Sun, Qiong Tang, Kuanning Wang, Xuanjing Huang, and Xipeng Qiu. Dif-
 601 fusionbert: Improving generative masked language models with diffusion models. In *ACL*, 2023.
- 602
- 603 Dan Hendrycks, Collin Burns, Saurav Kadavath, Akul Arora, Steven Basart, Eric Tang, Dawn
 604 Song, and Jacob Steinhardt. Measuring mathematical problem solving with the math dataset.
 605 In *NeurIPS*, 2021.
- 606
- 607 Jonathan Ho and Tim Salimans. Classifier-free diffusion guidance. In *NeurIPS*, 2021.
- 608
- 609 Jonathan Ho and Tim Salimans. Progressive distillation for fast sampling of diffusion models. In
 610 *ICLR*, 2022.
- 611
- 612 Chihang Huang and Hao Tang. Ctrlldiff: Boosting large diffusion language models with dynamic
 613 block prediction and controllable generation. *arXiv preprint arXiv:2505.14455*, 2025.
- 614
- 615 Albert Q. Jiang, Alexandre Sablayrolles, Arthur Mensch, Chris Bamford, Devendra Singh Chap-
 616 lot, Diego de las Casas, Florian Bressand, Gianna Lengyel, Guillaume Lample, Lucile Saulnier,
 617 Lélio Renard Lavaud, Marie-Anne Lachaux, Pierre Stock, Teven Le Scao, Thibaut Lavril, Thomas
 618 Wang, Timothée Lacroix, and William El Sayed. Mistral 7b. *arXiv preprint arXiv:2310.06825*,
 619 2023.
- 620
- 621 Nirmit Joshi, Gal Vardi, Adam Block, Surbhi Goel, Zhiyuan Li, Theodor Misiakiewicz, and Nathan
 622 Srebro. A theory of learning with autoregressive chain of thought. In *COLT*, 2025.
- 623
- 624 Rabeeh Karimi Mahabadi, Hamish Ivison, Jaesung Tae, James Henderson, Iz Beltagy, Matthew E.
 625 Peters, and Arman Cohan. Tess: Text-to-text self-conditioned simplex diffusion. In *EACL*, 2024.
- 626
- 627 Torben Knappe, Yanzhe Li, Ankit Chauhan, Pranay Oruganti, Hannaneh Hajishirzi, and Sameer
 628 Singh. Semantic self-consistency: Enhancing language model reasoning via semantic weighting.
 629 In *NeurIPS*, 2024.
- 630
- 631 Philipp Koehn and Rebecca Knowles. Six Challenges for Neural Machine Translation. In *ACL
 632 Workshop*, 2017.
- 633
- 634 Takeshi Kojima, Shixiang Gu, Machel Reid, Yutaka Matsuo, and Yusuke Iwasawa. Large language
 635 models are zero-shot reasoners. In *NeurIPS*, 2022.
- 636
- 637 Vijay Korthikanti, Mostofa Patwary, Reza Yazdani Aminabadi, Ammar Ahmad Awan, Samyam Ra-
 638 jibhandari, Cheng Li, Eric Zheng, Shiming Li, Zhao Song, Yuxiong He, Trishul Chilimbi, Haibin
 639 Fu, Michael Smith, Mohammad Shoeybi, and Bryan Catanzaro. Reducing activation recomputa-
 640 tion in large transformer models. In *MLSys*, 2022.
- 641
- 642 Adarsh Kumar, Hwiyoon Kim, Jawahar Sai Nathani, and Neil Roy. Improving the reliability of llms:
 643 Combining cot, rag, self-consistency, and self-verification. *arXiv preprint arXiv:2505.09031*,
 2025.
- 644
- 645 Sangyun Lee, Zinan Lin, and Giulia Fanti. Improving the training of rectified flows. In *NeurIPS*,
 646 2024.
- 647
- 648 Xiang Lisa Li, Tianhao Gao, Yizhong Chen, Karthik Narasimhan, Percy Liang, and Tatsunori B.
 649 Hashimoto. Diffusion-lm improves controllable text generation. In *NeurIPS*, 2022.
- 650
- 651 Yaron Lipman, Ricky T. Q. Chen, Heli Ben-Hamu, Maximilian Nickel, and Matthew Le. Flow
 652 matching for generative modeling. In *ICLR*, 2023.
- 653
- 654 Jian Liu, Leyang Cui, Hanmeng Liu, Dandan Huang, Yile Wang, and Yue Zhang. LogiQA: A
 655 challenge dataset for machine reading comprehension with logical reasoning. In *IJCAI*, 2020.

- 648 Jin Liu and Steffen Thoma. Fzi-wim at semeval-2024 task 2: Self-consistent cot for complex nli in
 649 biomedical domain. In *NAACL Workshop*, 2024.
- 650
- 651 Zhiyuan Liu, Yicun Yang, Yaojie Zhang, Junjie Chen, Chang Zou, Qingyuan Wei, Shaobo Wang,
 652 and Linfeng Zhang. dilm-cache: Accelerating diffusion large language models with adaptive
 653 caching. *arXiv preprint arXiv:2506.06295*, 2025.
- 654 Justin Lovelace, Varsha Kishore, Chao Wan, Eliot Shekhtman, and Kilian Q Weinberger. Latent
 655 diffusion for language generation. In *NeurIPS*, 2023.
- 656
- 657 Todor Mihaylov, Peter Clark, Tushar Khot, and Ashish Sabharwal. Can a suit of armor conduct
 658 electricity? a new dataset for open book question answering. In *EMNLP*, 2018.
- 659
- 660 Deepak Narayanan, Mohammad Shoeybi, Jared Casper, Patrick LeGresley, Mostofa Patwary, Vi-
 661 jay Korthikanti, Dmitri Vainbrand, Prethvi Kashinkunti, Julie Bernauer, Bryan Catanzaro, Amar
 662 Phanishayee, and Matei Zaharia. Efficient large-scale language model training on gpu clusters
 663 using megatron-Im. In *SC*, 2021.
- 664
- 665 Shen Nie, Fengqi Zhu, Zebin You, Xiaolu Zhang, Jingyang Ou, Jun Hu, Jun Zhou, Yankai
 666 Lin, Ji-Rong Wen, and Chongxuan Li. Large language diffusion models. *arXiv preprint*
 667 *arXiv:2502.09992*, 2025.
- 668
- 669 Yixin Nie, Adina Williams, Emily Dinan, Mohit Bansal, Jason Weston, and Douwe Kiela. Adver-
 670 sarial NLI: A new benchmark for natural language understanding. In *ACL*, 2020.
- 671
- 672 Long Ouyang, Jeff Wu, Xu Jiang, Diogo Almeida, Carroll Wainwright, Pamela Mishkin, Chong
 673 Zhang, Sandhini Agarwal, Katarina Slama, Alex Ray, John Schulman, Jacob Hilton, Fraser Kel-
 674 ton, Luke Miller, Maddie Simens, Amanda Askell, Peter Welinder, Paul Christiano, Jan Leike, and
 675 Ryan Lowe. Training language models to follow instructions with human feedback. In *NeurIPS*,
 676 2022.
- 677
- 678 Adam Paszke, Sam Gross, Francisco Massa, Adam Lerer, James Bradbury, Gregory Chanan, Trevor
 679 Killeen, Zeming Lin, Natalia Gimelshein, Luca Antiga, Alban Desmaison, Andreas Kopf, Edward
 680 Yang, Zachary DeVito, Martin Raison, Alykhan Tejani, Sasank Chilamkurthy, Benoit Steiner,
 681 Lu Fang, Junjie Bai, and Soumith Chintala. Pytorch: An imperative style, high-performance deep
 682 learning library. In *NeurIPS*, 2019.
- 683
- 684 Yao Qiang, Subhrangshu Nandi, Ninareh Mehrabi, Greg Ver Steeg, Anoop Kumar, Anna Rumshisky,
 685 and Aram Galstyan. Prompt perturbation consistency learning for robust language models. In
 686 *EACL*, 2024.
- 687
- 688 Samyam Rajbhandari, Olatunji Ruwase, Jeff Rasley, and Yuxiong He. Zero: Memory optimizations
 689 toward training trillion parameter models. In *SC*, 2020.
- 690
- 691 Marc'Aurelio Ranzato, Sumit Chopra, Michael Auli, and Wojciech Zaremba. Sequence Level Train-
 692 ing with Recurrent Neural Networks. In *ICLR*, 2016.
- 693
- 694 Matthew Renze. The effect of sampling temperature on problem solving in large language models.
 695 In *EMNLP*, 2024.
- 696
- 697 Melissa Roemmele, Cosmin Adrian Bejan, and Andrew S. Gordon. Choice of plausible alternatives:
 698 An evaluation of commonsense causal reasoning. In *AAAI*, 2011.
- 699
- 700 Subham S. Sahoo, Marianne Arriola, Yair Schiff, Aaron Gokaslan, Edgar Marroquin, Justin T. Chiu,
 701 Alexander Rush, and Volodymyr Kuleshov. Simple and effective masked diffusion language
 702 models. In *NeurIPS*, 2024.
- 703
- 704 Subham Sekhar Sahoo, Justin Deschenaux, Aaron Gokaslan, Guanghan Wang, Justin Chiu, and
 705 Volodymyr Kuleshov. The diffusion duality. *arXiv preprint arXiv:2506.10892*, 2025.
- 706
- 707 Tim Salimans, Thomas Mensink, Jonathan Heek, and Emiel Hoogeboom. Multistep distillation of
 708 diffusion models via moment matching. In *NeurIPS*, 2024.
- 709
- 710 Florian Schmidt. Generalization in Generation: A Closer Look at Exposure Bias. In *EMNLP*, 2019.

- 702 Andy Shih, Dorsa Sadigh, and Stefano Ermon. Long horizon temperature scaling. In *ICML*, 2023.
 703
- 704 Yang Song and Prafulla Dhariwal. Improved techniques for training consistency models. In *ICLR*,
 705 2024.
- 706 Yang Song, Prafulla Dhariwal, Mark Chen, and Ilya Sutskever. Consistency models. In *ICML*, 2023.
 707
- 708 Zayne Sprague, Fangcong Yin, Juan Diego Rodriguez, Dongwei Jiang, Manya Wadhwa, Prasann
 709 Singhal, Xinyu Zhao, Xi Ye, Kyle Mahowald, and Greg Durrett. To CoT or not to CoT? chain-
 710 of-thought helps mainly on math and symbolic reasoning. In *ICLR*, 2025.
- 711 Mirac Suzgun, Nathan Scales, Nathanael Schärl, Sebastian Gehrmann, Yi Tay, Hyung Won Chung,
 712 Aakanksha Chowdhery, Quoc V. Le, Denny Zhou, and Jason Wei. Challenging big-bench tasks
 713 and whether chain-of-thought can solve them. In *ICLR*, 2023.
 714
- 715 Hugo Touvron, Thibaut Lavril, Gautier Izacard, Xavier Martinet, Marie-Anne Lachaux, Timothée
 716 Lacroix, Baptiste Rozière, Naman Goyal, Eric Hambro, Faisal Azhar, Aurélien Rodriguez, Ar-
 717 mand Joulin, Edouard Grave, and Guillaume Lample. Llama: Open and efficient foundation
 718 language models. *arXiv preprint arXiv:2302.13971*, 2023.
- 719 Harshit Varma, Dheeraj Nagaraj, and Karthikeyan Shanmugam. Glauber generative model: Discrete
 720 diffusion models via binary classification. In *ICLR*, 2025.
- 721 Ashish Vaswani, Noam Shazeer, Niki Parmar, Jakob Uszkoreit, Llion Jones, Aidan N. Gomez,
 722 Łukasz Kaiser, and Illia Polosukhin. Attention is all you need. In *NeurIPS*, 2017.
- 723 Ashwin K Vijayakumar, Michael Cogswell, Ramprasaath R Selvaraju, Qing Sun, Stefan Lee, David
 724 Crandall, and Dhruv Batra. Diverse Beam Search: Decoding Diverse Solutions from Neural
 725 Sequence Models. In *AAAI*, 2018.
- 726 Fu-Yun Wang, Ling Yang, Zhaoyang Huang, Mengdi Wang, and Hongsheng Li. Rectified diffusion:
 727 Straightness is not your need in rectified flow. In *ICLR*, 2025a.
- 728 Guanzhi Wang, Yuqi Xie, Yunfan Jiang, Ajay Mandlekar, Chaowei Xiao, Yuke Zhu, Linxi Fan, and
 729 Anima Anandkumar. Voyager: An open-ended embodied agent with large language models. In
 730 *TMLR*, 2023a.
- 731 Hongru Wang, Deng Cai, Wanjun Zhong, Shijue Huang, Jeff Z. Pan, Zeming Liu, and Kam-Fai
 732 Wong. Self-Reasoning Language Models: Unfold Hidden Reasoning Chains with Few Reasoning
 733 Catalyst. *arXiv preprint arXiv:2505.14116*, 2025b.
- 734 Jin Wang, Yao Lai, Aoxue Li, Shifeng Zhang, Jiacheng Sun, Ning Kang, Chengyue Wu, Zhenguo
 735 Li, and Ping Luo. Fudoki: Discrete flow-based unified understanding and generation via kinetic-
 736 optimal velocities. *arXiv preprint arXiv:2505.20147*, 2025c.
- 737 Weiqin Wang, Yile Wang, and Hui Huang. Ranked voting based self-consistency of large language
 738 models. In *ACL*, 2025d.
- 739 Xuezhi Wang, Jason Wei, Dale Schuurmans, Quoc V. Le, Ed H. Chi, and Denny Zhou. Self-
 740 consistency improves chain of thought reasoning in language models. In *ICLR*, 2023b.
- 741 Jason Wei, Xuezhi Wang, Dale Schuurmans, Maarten Bosma, Brian Ichter, Fei Xia, Ed H. Chi,
 742 Quoc V. Le, and Denny Zhou. Chain-of-thought prompting elicits reasoning in large language
 743 models. In *NeurIPS*, 2022.
- 744 Adina Williams, Nikita Nangia, and Samuel R. Bowman. A broad-coverage challenge corpus for
 745 sentence understanding through inference. In *NAACL*, 2018.
- 746 Chengyue Wu, Hao Zhang, Shuchen Xue, Zhijian Liu, Shizhe Diao, Ligeng Zhu, Ping Luo, Song
 747 Han, and Enze Xie. Fast-dllm: Training-free acceleration of diffusion llm by enabling kv cache
 748 and parallel decoding. *arXiv preprint arXiv:2505.22618*, 2025.
- 749 Yangzhen Wu, Zhiqing Sun, Shanda Li, Sean Welleck, and Yiming Yang. An empirical analysis of
 750 compute-optimal inference for problem-solving with language models. In *NeurIPS*, 2024a.

- 756 Zhenyu Wu, Qingkai Zeng, Zhihan Zhang, Zhaoxuan Tan, Chao Shen, and Meng Jiang. Large
 757 language models can self-correct with key condition verification. In *EMNLP*, 2024b.
 758
- 759 Sirui Xie, Zhisheng Xiao, Diederik P. Kingma, Tingbo Hou, Ying Nian Wu, Kevin P. Murphy, Tim
 760 Salimans, Ben Poole, and Ruiqi Gao. EM distillation for one-step diffusion models. In *NeurIPS*,
 761 2024.
- 762 Yida Xiong, Kun Li, Jiameng Chen, Hongzhi Zhang, Di Lin, Yan Che, and Wenbin Hu. Text-
 763 guided multi-property molecular optimization with a diffusion language model. *arXiv preprint*
 764 *arXiv:2410.13597*, 2024.
- 765 Minkai Xu, Tomas Geffner, Karsten Kreis, Weili Nie, Yilun Xu, Jure Leskovec, Stefano Ermon, and
 766 Arash Vahdat. Energy-based diffusion language models for text generation. In *ICLR*, 2025.
- 768 Ling Yang, Ye Tian, Bowen Li, Xinchen Zhang, Ke Shen, Yunhai Tong, and Mengdi Wang. Mmada:
 769 Multimodal large diffusion language models. *arXiv preprint arXiv:2505.15809*, 2025.
- 771 Shunyu Yao, Dian Yu, Jeffrey Zhao, Izhak Shafran, Tom Griffiths, Yuan Cao, and Karthik
 772 Narasimhan. Tree of thoughts: Deliberate problem solving with large language models. In
 773 *NeurIPS*, 2023.
- 774 Jiacheng Ye, Shansan Gong, Liheng Chen, Lin Zheng, Jiahui Gao, Han Shi, Chuan Wu, Zhenguo
 775 Li, Wei Bi, and Lingpeng Kong. Diffusion of thoughts: Chain-of-thought reasoning in diffusion
 776 language models. In *Neurips*, 2024.
- 778 Jiacheng Ye, Jiahui Gao, Shansan Gong, Lin Zheng, Xin Jiang, Zhenguo Li, and Lingpeng Kong.
 779 Beyond Autoregression: Discrete Diffusion for Complex Reasoning and Planning. In *ICLR*,
 780 2025a.
- 781 Jiacheng Ye, Zihui Xie, Lin Zheng, Jiahui Gao, Zirui Wu, Xin Jiang, Zhenguo Li, and Lingpeng
 782 Kong. Dream 7b: Diffusion large language models. *arXiv preprint arXiv:2508.15487*, 2025b.
- 784 Zebin You, Shen Nie, Xiaolu Zhang, Jun Hu, Jun Zhou, Zhiwu Lu, Ji-Rong Wen, and Chongxuan
 785 Li. Llada-v: Large language diffusion models with visual instruction tuning. *arXiv preprint*
 786 *arXiv:2505.16933*, 2025.
- 787 Fei Yu, Hongbo Zhang, Prayag Tiwari, and Benyou Wang. Natural language reasoning, a survey.
 788 *ACM Computing Surveys*, 56(7):1–36, 2024.
- 790 Qifan Yu, Zhenyu He, Sijie Li, Xun Zhou, Jun Zhang, Jingjing Xu, and Di He. Enhancing auto-
 791 regressive chain-of-thought through loop-aligned reasoning. *arXiv preprint arXiv:2502.08482*,
 792 2025.
- 793 Eric Zelikman, Yuhuai Wu, and Noah D. Goodman. Star: Bootstrapping reasoning with reasoning.
 794 In *NeurIPS*, 2022.
- 796 Rowan Zellers, Ari Holtzman, Yonatan Bisk, Ali Farhadi, and Yejin Choi. Hellaswag: Can a ma-
 797 chine really finish your sentence? In *ACL*, 2020.
- 798 Andy Zeng, Maria Attarian, Brian Ichter, Krzysztof Marcin Choromanski, Adrian Wong, Stefan
 799 Welker, Federico Tombari, Aveek Purohit, Michael S. Ryoo, Vikas Sindhwani, Johnny Lee, Vin-
 800 cent Vanhoucke, and Pete Florence. Socratic models: Composing zero-shot multimodal reasoning
 801 with language. In *ICLR*, 2023.
- 803 Shimao Zhang, Yu Bao, and Shujian Huang. Edt: Improving large language models’ generation by
 804 entropy-based dynamic temperature sampling. *arXiv preprint arXiv:2403.14541*, 2024a.
- 805 Xiang Zhang, Muhammad Abdul-Mageed, and Laks VS Lakshmanan. Autoregressive+ chain of
 806 thought= recurrent: Recurrence’s role in language models’ computability and a revisit of recurrent
 807 transformer. *arXiv preprint arXiv:2409.09239*, 2024b.
- 809 Zhuosheng Zhang, Aston Zhang, Mu Li, and Alex Smola. Automatic chain of thought prompting in
 large language models. In *ICLR*, 2023.

- 810 Ziqi Zhang, Cunxiang Wang, Xiao Xiong, Yue Zhang, and Donglin Wang. Nash cot: Multi-path
811 inference with preference equilibrium. In *EMNLP*, 2024c.
812
- 813 Siyan Zhao, Devaansh Gupta, Qinqing Zheng, and Aditya Grover. d1: Scaling Reasoning in Diffu-
814 sion Large Language Models via Reinforcement Learning. In *NeurIPS*, 2025.
815
- 816 Lin Zheng, Jianbo Yuan, Lei Yu, and Lingpeng Kong. A reparameterized discrete diffusion model
817 for text generation. *arXiv preprint arXiv:2302.05737*, 2023.
818
- 819 Denny Zhou, Nathanael Schärli, Le Hou, Jason Wei, Nathan Scales, Xuezhi Wang, Dale Schu-
820 urmans, Claire Cui, Olivier Bousquet, Quoc V. Le, and Ed H. Chi. Least-to-most prompting
821 enables complex reasoning in large language models. In *ICLR*, 2023.
822
- 823 Kun Zhou, Yifan Li, Wayne Xin Zhao, and Ji-Rong Wen. Diffusion-nat: Self-prompting discrete
824 diffusion for non-autoregressive text-to-text generation. In *EACL*, 2024a.
825
- 826 Mingyuan Zhou, Huangjie Zheng, Zhendong Wang, Mingzhang Yin, and Hai Huang. Score identity
827 distillation: Exponentially fast distillation of pretrained diffusion models for one-step generation.
828 In *ICML*, 2024b.
829
- 830 Fengqi Zhu, Rongzhen Wang, Shen Nie, Xiaolu Zhang, Chunwei Wu, Jun Hu, Jun Zhou, Jianfei
831 Chen, Yankai Lin, Ji-Rong Wen, and Chongxuan Li. Llada 1.5: Variance-reduced preference
832 optimization for large language diffusion models. *arXiv preprint arXiv:2505.19223*, 2025a.
833
- 834 Yuanzhi Zhu, Xingchao Liu, and Qiang Liu. Slimflow: Training smaller one-step diffusion models
835 with rectified flow. In *ECCV*, 2024.
836
- 837 Yuanzhi Zhu, Xi Wang, Stéphane Lathuilière, and Vicky Kalogeiton. Di[m]o: Distilling masked
838 diffusion models into one-step generator. *arXiv preprint arXiv:2503.15457*, 2025b.
839
- 840
- 841
- 842
- 843
- 844
- 845
- 846
- 847
- 848
- 849
- 850
- 851
- 852
- 853
- 854
- 855
- 856
- 857
- 858
- 859
- 860
- 861
- 862
- 863

864

SUMMARY OF THE APPENDIX

865

866 This appendix contains additional details for the ICLR 2026 submission, titled “*Beyond Next-Token*
 867 *Prediction: Diffusion vs. Autoregressive Reasoning in LLMs*”. The appendix is organized as follows:

868

- §S1 introduces the **datasets**, covering statistics, task categories, and evaluation metrics.
- §S2 reports **additional results**, and shows radar charts that compare models across benchmarks.
- §S3 presents **failure cases in single-constraint tasks** and explains why AR LLMs outperform DLLMs in these settings.
- §S4 presents **failure cases in multi-constraint tasks** and shows that DLLMs outperform AR LLMs when multiple interdependent constraints must be satisfied.
- §S5 provides an **analysis of efficiency scaling**, and reports memory usage and latency as a function of sequence length for AR and DLLMs.
- §S7 provides an **examination of test-time scaling**, and compares AR LLMs with beam search.
- §S9 offers a **summary of licenses and consent**, and lists usage terms for all models and datasets.
- §S10 provides a **discussion of social impact and limitations**, and highlights broader implications and open challenges.
- §S11 provides an **AI disclosure**, and notes that AI assistance was limited to grammar checking.

881

S1 DATASETS AND EVALUATION METRICS

882

S1.1 DATASETS

883

884 We evaluate our models on a broad set of benchmarks spanning mathematical reasoning, natural
 885 language inference, logical reasoning, and commonsense question answering. Below we provide
 886 dataset descriptions and links for reproducibility.

887

Mathematical reasoning.

888

- **GSM8K** (Cobbe et al., 2021): a grade school math word problem benchmark. Available at <https://huggingface.co/datasets/openai/gsm8k>.
- **MathQA** (Amini et al., 2019): a collection of math word problems derived from AQuA. Available at https://huggingface.co/datasets/allenai/math_qa.
- **Minerva Math** (Hendrycks et al., 2021): a large-scale dataset covering 7 sub-fields of mathematics. Available at https://huggingface.co/datasets/EleutherAI/hendrycks_math.

889

Natural language inference.

900

- **ANLI** (Nie et al., 2020): an adversarially collected NLI benchmark. Available at <https://huggingface.co/datasets/facebook/anli>.
- **MNLI** (Williams et al., 2018): a broad-coverage NLI dataset. Available at <https://huggingface.co/datasets/nyu-mll/glue>.
- **RTE** (Williams et al., 2018): a textual entailment dataset from the GLUE benchmark. Available at <https://huggingface.co/datasets/nyu-mll/glue>.

908

Logical reasoning.

910

- **LSAT-LR**: logical reasoning problems from the LSAT exam. Available at <https://huggingface.co/datasets/hails/agieval-lsat-lr>.
- **LogiQA-en** (Liu et al., 2020): an English logical reasoning benchmark. Available at <https://huggingface.co/datasets/hails/agieval-logiqa-en>.

911

Commonsense QA.

912

- **COPA** (Roemmele et al., 2011): a causal reasoning dataset. Available at https://huggingface.co/datasets/super_glue/viewer/copa.

- 918
 919
 920 • **PIQA** (Bisk et al., 2020): a physical commonsense reasoning benchmark. Available at
 921 <https://huggingface.co/datasets/ybisk/piqa>.
 922 • **OpenBookQA** (Mihaylov et al., 2018): multiple-choice science QA benchmark. Available
 923 at <https://huggingface.co/datasets/allenai/openbookqa>.
 924 • **HellaSwag** (Zellers et al., 2020): commonsense completion benchmark with adver-
 925 sarial filtering. Available at <https://huggingface.co/datasets/Rowan/hellaswag>.
 926
 927

928 **S1.2 EVALUATION METRICS**
 929

930 For **mathematical reasoning tasks** (GSM8K, MathQA, Minerva Math), we use *Exact Match (EM)*
 931 accuracy. We consider both strict and flexible EM (the latter allows normalization such as removing
 932 commas, units, and checking mathematical equivalence, *e.g.*, $0.5 = 1/2$), as well as Math Verify
 933 (MV) for Minerva Math. Following standard practice, we report the highest score among these
 934 metrics for each dataset to ensure comparability with prior work.

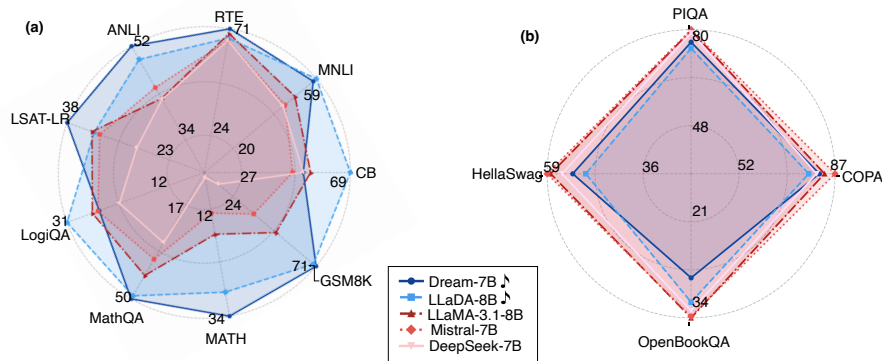
935 For **natural language inference tasks** (ANLI, MNLI, RTE), we use *classification accuracy*, *i.e.*,
 936 the percentage of samples where the predicted label exactly matches the gold label.

937 For **multiple-choice QA tasks** (LSAT-LR, LogiQA-en, COPA, PIQA, OpenBookQA, HellaSwag),
 938 we use *multiple-choice accuracy*, defined as the proportion of questions where the correct option is
 939 selected. We primarily report standard accuracy in the main paper for consistency.

940 For **multi-subtask datasets** (Minerva Math, ANLI), accuracy is first computed per subtask and then
 941 aggregated using sample-weighted averages. This weighting reflects the relative size of each subtask
 942 and avoids distortions from smaller subsets.

943 All metrics are case-insensitive and allow minor formatting variations through regex-based normal-
 944 ization. In practice, this normalization accounts for superficial differences such as spacing, capital-
 945 ization, or symbol usage.

946
 947 **S2 ADDITIONAL RESULTS**
 948



949
 950 Figure S1: **Radar charts of five models.** (a) Tasks where AR LLMs outperform DLLMs. (b) Tasks
 951 where DLLMs outperform AR LLMs.
 952

953 **AR advantages.** On commonsense QA benchmarks such as PIQA, HellaSwag, COPA, and Open-
 954 BookQA, AR LLMs consistently achieve the best performance. For instance, Mistral-7B reaches
 955 80.2% on PIQA and 91.0% on COPA, clearly outperforming diffusion-based models. These results
 956 suggest that AR decoding remains more effective on short-context multiple-choice tasks where local
 957 token dependencies dominate.

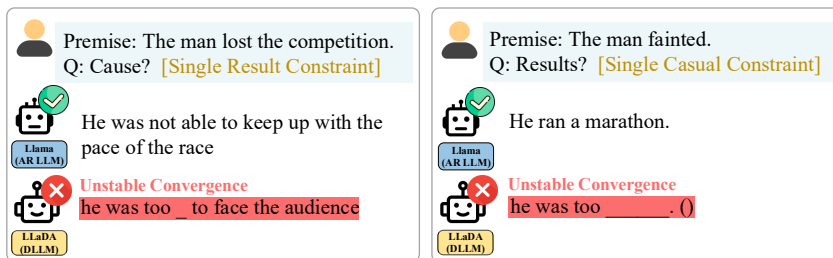
958 **DLLM advantages.** In contrast, DLLMs (Dream-7B and LLaDA-8B) show strong gains on multi-
 959 step reasoning datasets such as GSM8K, MathQA, and RTE. Dream-7B reaches 71.5% on GSM8K

972 and 50.0% on MathQA, surpassing AR counterparts by large margins. This highlights DLLMs' 973 strength in handling structured reasoning under multiple interdependent constraints. 974

975 DLLMs achieve consistent advantages on benchmarks that demand strong global consistency and 976 multi-step reasoning, where iterative refinement enables error correction and coherence. By contrast, 977 AR LLMs remain competitive on short-context commonsense QA, where fast left-to-right decoding 978 is sufficient for capturing single causal links and maintaining reasoning chains. 979

980 S3 FAILURE CASES IN SINGLE-CONSTRAINT TASKS 981

982 **Finding: Autoregressive models wins on single-constraint reasoning.** When tasks are driven by 983 *one dominant causal or procedural relation*, as in commonsense and procedural QA, AR LLMs 984 perform better. Left-to-right decoding ($p(x) = \prod_i p(x_i | x_{<i})$) constructs a stable and interpretable 985 chain, where each step relies directly on the previous one. This concentrates probability mass on the 986 “next sensible step,” reducing uncertainty and avoiding iterative dilution. Such single-pass reasoning 987 aligns well with single-constraint tasks. As shown in Fig. S1(a), AR LLMs achieve higher accuracy 988 on PIQA, COPA, OpenBookQA and Hellaswag. 989



990 Figure S2: **Autoregression outperforms diffusion on single-constraint reasoning.** Examples 991 from commonsense reasoning tasks show that Llama (AR) provides coherent causal links, while 992 LLaDA (DLLM) produces incomplete or redundant reasoning, illustrating difficulties in converging 993 on discrete cause–effect constraints. 994

1000 While DLLMs excel at multi-constraint reasoning, they often underperform AR LLMs on single- 1001 constraint tasks. Figure S2 shows two representative examples from commonsense reasoning 1002 benchmarks. Autoregressive models generate tokens causally, which enforces strong local coherence. This 1003 makes them effective when solving problems reducible to a single causal link (e.g., identifying a 1004 direct cause or a single plausible outcome). As seen in the examples, Llama produces fluent and 1005 consistent explanations such as “he was not able to keep up with the pace of the race.” In 1006 contrast, DLLMs rely on bidirectional denoising, which weakens causal flow and may yield incomplete 1007 fragments rather than converging on the correct relation. 1008

1009 As a result, DLLMs sometimes generate incomplete fragments (“he was too _ to face the audience”), 1010 failing to capture the intended causal relation. This reflects a general weakness of DLLMs in tasks 1011 where precision hinges on a single constraint. 1012

1015 S4 ADDITIONAL FAILURE CASE ANALYSES IN MUTI-CONSTRAINT TASKS 1016

1017 We provide further failure case analyses to complement the main text. Figure S3 illustrates four 1018 multi-constraint tasks where diffusion consistently outperforms autoregression. 1019

1020 In Fig. S3(a), Llama (AR LLM) ignores constraints 1 and 2, producing inconsistent arithmetic, while 1021 LLaDA (DLLM) satisfies all quantitative conditions. In Fig. S3(b), Llama fails to account for the 1022 temporal relation (2011 vs. 2008), whereas LLaDA preserves lexical consistency. In Fig. S3(c), 1023 Llama omits the total-sum requirement in a story aggregation task, but LLaDA produces the correct 1024 outcome. In Fig. S3(d), Llama misreads the average constraint as a daily increment, leading to 1025 compounding errors, while LLaDA maintains global coherence.

1026 These additional cases further demonstrate DLLMs’ ability to maintain global consistency under 1027 multi-constraint reasoning. 1028



Figure S3: DLLMs win on multi-constraint reasoning.

S5 EFFICIENCY

A critical dimension differentiating reasoning paradigms is computational efficiency, particularly latency and memory consumption, which directly impact practical deployment. We conducted stress tests on both LLaDA (DLLM) and Llama (AR LLM) across varying sequence lengths.

As shown in Table S1, Llama's latency remains nearly constant (5–6s) across prompt lengths from 32 to 2048 tokens, indicating near-linear scalability. In contrast, LLaDA exhibits sharp latency growth: from 11.2s at 32 tokens to 62.8s at 2048 tokens. This divergence reflects the fundamental difference between paradigms: AR decoding processes tokens sequentially with stable cost per step, while diffusion-based decoding incurs iterative refinement, with costs rising sharply as context length grows. This shows DLLMs face challenges in handling long contexts efficiently.

This analysis confirms a fundamental trade-off: the reasoning strengths of DLLMs come at a significant cost in terms of computational efficiency, whereas AR LLM offer a much more scalable and resource-friendly solution, making them better suited for real-time or resource-constrained applications. Deploying diffusion decoding therefore requires careful attention to latency despite its accuracy and robustness gains.

1080 Table S1: **Latency as a function of prompt length.** Llama’s cost remains stable, while LLaDA
 1081 grows sharply with longer prompts. Latency is measured in seconds.
 1082

Prompt Length	Llama-3.1-8B	LLaDA-8B
32	5.5	11.2
64	5.5	11.5
128	5.6	12.1
256	5.6	15.3
512	5.7	21.1
1024	5.7	35.9
2048	5.7	62.8

1093 This analysis confirms a fundamental trade-off: the reasoning strengths of DLLMs come at a sig-
 1094 nificant cost in terms of computational efficiency, whereas AR LLM offer a much more scalable
 1095 and resource-friendly solution, making them better suited for real-time or resource-constrained ap-
 1096 plications. Deploying diffusion decoding therefore requires careful attention to latency despite its
 1097 accuracy and robustness gains.

1098 Table S2 compares end-to-end inference latency across benchmarks, normalized to Llama-3.1-8B.
 1099 We find that diffusion decoding is consistently slower, often by $4\times$ – $43\times$, depending on the number
 1100 of denoising steps. For instance, on GSM8K, Dream-7B is $25.9\times$ slower, and LLaDA-8B is $27.4\times$
 1101 slower. This highlights the key bottleneck of current diffusion LLMs: while they improve reasoning
 1102 accuracy, their practical deployment is limited by inference speed (Li et al., 2022).
 1103

1104 Table S2: **Latency comparison** across different tasks relative to Llama-3.1-8B.

Models	DLLM		AR LLM		
	Dream	LLaDA	Llama	Mistral	DeepSeek
Parameter	7B	8B	8B	7B	7B
Mathematical Reasoning					
GSM8K	25.9 \times	27.4 \times	1.0 \times	0.5 \times	0.4 \times
MathQA	15.5 \times	17.4 \times	1.0 \times	1.0 \times	1.0 \times
Minerva Math	15.6 \times	17.6 \times	1.0 \times	0.7 \times	0.7 \times
Natural Language Inference/QA					
MNLI	3.3 \times	3.9 \times	1.0 \times	0.9 \times	1.1 \times
RTE	9.7 \times	9.8 \times	1.0 \times	1.0 \times	1.0 \times
QQP	5.3 \times	5.3 \times	1.0 \times	1.0 \times	1.0 \times
ANLI	17.9 \times	18.0 \times	1.0 \times	1.1 \times	1.1 \times
Logical Reasoning					
LSAT-LR	38.8 \times	43.0 \times	1.0 \times	1.1 \times	1.0 \times
LogiQA-en	32.0 \times	37.2 \times	1.0 \times	1.1 \times	1.0 \times
Commonsense QA Reasoning					
COPA	5.6 \times	4.5 \times	1.0 \times	1.0 \times	0.9 \times
PIQA	6.9 \times	6.4 \times	1.0 \times	1.1 \times	1.0 \times
OpenBookQA	9.5 \times	9.4 \times	1.0 \times	1.1 \times	1.0 \times
HellaSwag	17.3 \times	11.2 \times	1.0 \times	1.0 \times	0.9 \times

1125

S6 COT RESULTS

1126 Table S3 reports Math Verify (MV) accuracy for LLaDA-8B (DLLM) and Llama-3.1-8B (AR) on
 1127 the Minerva MATH sub-tasks, both with and without CoT prompting.
 1128

1129 For DLLMs, CoT generally fails to provide improvements and sometimes lowers accuracy (*e.g.*,
 1130 Algebra 41.5 → 40.0, Number Theory 22.8 → 19.8). In contrast, AR LLMs show modest but
 1131 consistent gains from CoT in several sub-tasks (*e.g.*, Prealgebra 33.8 → 38.6, Geometry 11.3 →
 1132 13.6). This suggests that iterative refinement in DLLMs already supports multi-step reasoning, so
 1133 external CoT scaffolding can interfere with their decoding process.

1134 Table S3: **CoT prompting on Minerva Math sub-tasks.** Math Verify (MV) accuracy (%).
1135

Sub-task	LLaDA-8B (DLLM) w/o CoT	LLaDA-8B (DLLM) w/ CoT	Llama-3.1-8B (AR LLM) w/o CoT	Llama-3.1-8B (AR LLM) w/ CoT
Algebra	41.5	40.0	27.7	29.3
Counting & Prob.	25.9	23.0	17.1	16.2
Geometry	19.8	18.4	11.3	13.6
Intermediate Algebra	9.7	9.4	6.2	7.3
Number Theory	22.8	19.8	9.6	9.6
Prealgebra	50.1	51.7	33.8	38.6
Precalculus	11.4	12.8	7.5	8.4

1144
1145 AR LLMs show consistent gains from CoT, while DLLMs exhibit limited or negative response. This
1146 suggests that CoT prompting (Wei et al., 2022; Kojima et al., 2022) is more effective for AR LLMs,
1147 whereas DLLMs do not benefit under the same setting.

1149 S7 ADDITIONAL RESULTS ON TEST-TIME SCALING

1151
1152 **Beam search analysis.** We further evaluate the effect of beam search (a common test-time scaling
1153 method (Vijayakumar et al., 2018; Koehn & Knowles, 2017)) on Llama (see Table S4). Specifically,
1154 we compare greedy decoding ($B = 1$) and beam widths of $B = 2, 4, 8$ on GSM8K. The accuracies
1155 are 50.2, 37.4, 38.5, and 37.7, respectively. Despite these adjustments, Llama consistently under-
1156 performs compared to diffusion-based models, indicating that simply enlarging the beam does not
1157 bridge the gap. This highlights that DLLMs' advantage is not attributable to insufficient search at
1158 test time, but rather to their inherent iterative refinement process.

1159 Table S4: **Effect of beam width on Llama vs. LLaDA (GSM8K accuracy).** Beam search does not
1160 improve AR performance; all settings remain below DLLMs.

Beam width (B)	Llama (AR LLM)	LLaDA (DLLM)
1 (greedy)	50.2	
2	37.4	
4	38.5	
8	37.7	70.7

1168 S8 FUTURE DIRECTIONS

1169 Our study highlights both the strengths and limitations of AR LLMs and DLLMs. Several promising
1170 directions emerge for advancing diffusion-based reasoning and hybrid architectures:

1171 **1. Sampling and Efficiency Optimization.** Current DLLMs still depend on dozens or even hun-
1172 dreds of denoising steps, which makes inference slow and resource-intensive. A key research di-
1173 rection is to design more efficient sampling strategies that reduce steps without degrading accuracy.
1174 One option is to adopt **adaptive noise schedules**, where the number of refinement steps is dyna-
1175 mically adjusted by token-level uncertainty. Another possibility is **budgeted DLLMs**, in which the
1176 model runs under a fixed compute or latency budget and applies early stopping once convergence
1177 is detected. In addition, methods such as progressive distillation, caching, or step-sharing across
1178 tokens may further accelerate decoding. Together, these approaches aim to close the gap between
1179 the reasoning ability of DLLMs and the efficiency required for deployment.

1180 **2. Hybrid AR-Diffusion LLMs Paradigms.** Recent work has already explored various forms
1181 of hybridization, such as Block Diffusion (Arriola et al., 2025), demonstrating that AR LLMs and
1182 DLLMs can complement each other.

1183 As illustrated in Figure S4, one practical pipeline is a two-stage process:

- 1184 1. **AR Seeding (Sketch Creation):** An autoregressive model generates an initial, syntac-
1185 tically sound draft, addressing DLLMs's weakness in maintaining tight local dependencies.

- 1188
 1189
 1190
 1191
 1192
 1193
 1194
 1195
 1196
 1197
 1198
 1199
 1200
 1201
 1202
 1203
 1204
 1205
 1206
 1207
 1208
 1209
 1210
 1211
 1212
 1213
 1214
 1215
 1216
 1217
 1218
 1219
 1220
 1221
 1222
 1223
 1224
 1225
 1226
 1227
 1228
 1229
 1230
 1231
 1232
 1233
 1234
 1235
 1236
 1237
 1238
 1239
 1240
 1241
2. **Diffusion Refinement (Global Improvement):** The AR output is then treated as a noisy-but-structured input for a DLLMs which iteratively refines the sequence to improve global logic and coherence.



Figure S4: **A Hybrid AR-Diffusion Architecture.** This model first uses an autoregressive transformer to generate a draft or “sketch” of discrete tokens (AR Seeding). This initial output is then fed into a DLLM for iterative refinement, improving global logic and coherence.

This architecture provides a concrete direction for hybrid reasoning systems. Another promising avenue is **task-adaptive routing**, where the decoder dynamically chooses between AR LLMs and DLLMs updates based on the structure of the problem.

3. Toward Unified Multimodal Reasoning. Diffusion provides a natural framework for multimodal reasoning because both discrete and continuous signals can be represented within the same denoising process. This opens the possibility of building LLMs that seamlessly integrate text, vision, and other modalities under a shared refinement cycle.

4. DLLMs as Agents. The bidirectional context, parallel decoding, and iterative refinement of DLLMs make them promising candidates for agentic applications. Unlike purely autoregressive models, DLLMs can plan and revise their outputs through repeated refinement, which resembles the cycle of planning, execution, and correction common in decision-making. This structure is particularly valuable in interactive environments. For example, an agent built on DLLMs could generate a tentative plan, refine it in response to feedback, and iteratively converge toward a reliable action sequence. Exploring this agentic potential may bridge the gap between static text generation and dynamic reasoning required in real-world tasks.

S9 ASSET LICENSE AND CONSENT

All models and datasets used in this work are publicly available. We strictly comply with their original licenses and use them only for non-commercial academic research. The contents of datasets do not represent our views or opinions.

Models. We evaluate five open-source models: Llama-3.1-8B (Meta custom license, attribution required, outputs may not be used to train competing models), Mistral-7B (Apache 2.0, permissive), DeepSeek-7B (DeepSeek custom license, attribution required), Dream-7B (Apache 2.0), and LLaDA-8B (MIT license). All licenses permit academic research use; detailed terms are available via the original model repositories.

Datasets. We use standard reasoning and QA benchmarks: GSM8K (MIT), MathQA (Apache 2.0), Minerva Math (MIT), ANLI (CC-BY-NC 4.0), MNLI (OANC + CC-BY-SA), RTE (GLUE permissive), LSAT-LR (MIT (via AGIEval)), LogiQA-en (CC-BY-NC-SA 4.0), COPA (CC-BY 4.0), PIQA (MIT), OpenBookQA (CC-BY-SA 3.0 for data, Apache 2.0 for code), and HellaSwag (CC-BY-NC 4.0). We note that some datasets include **non-commercial (NC)** and/or **share-alike (SA)** clauses; our use is strictly for academic purposes in compliance with these restrictions.

Consent. Our study does not involve crowdsourcing or human subjects. All results are derived from publicly available models and datasets.

1242 **S10 SOCIAL IMPACT AND LIMITATIONS**
12431244 Our study contributes to understanding how diffusion-based LLMs differ from autoregressive LLMs
1245 in reasoning, highlighting their relative strengths across task types. This provides insights into
1246 designing future reasoning models that better align with human-like problem solving.1247 However, several limitations remain. First, our evaluation focuses on a subset of reasoning tasks
1248 (mathematics, logic, commonsense, NLI), while broader domains such as multimodal reasoning
1249 (Driess et al., 2023; Achiam et al., 2023) and interactive agents (Wang et al., 2023a; Zeng
1250 et al., 2023) are not yet covered. Second, we mainly study mid-sized models (7B–8B), leaving open
1251 whether the relative advantages of DLLMs persist or amplify at larger scales (70B–100B). Third,
1252 our work does not introduce a concrete hybrid model that integrates AR and diffusion. A promising
1253 direction for future research is to design such a pipeline, where an AR LLM seeds a draft that is
1254 subsequently refined by diffusion.1255 Future work should therefore extend task coverage, validate scaling behavior, and develop practical
1256 hybrid pipelines that combine the strengths of both paradigms.
12571258 **S11 AI DISCLOSURE**
12591260 We acknowledge the use of GPT-5 for grammar checking only. The model was employed to correct
1261 grammatical errors while ensuring the original meaning and intent of the text remained unchanged.
1262
1263
1264
1265
1266
1267
1268
1269
1270
1271
1272
1273
1274
1275
1276
1277
1278
1279
1280
1281
1282
1283
1284
1285
1286
1287
1288
1289
1290
1291
1292
1293
1294
1295